ISSN 3048-8222 (Online) | www.ijsate.com | editor@ijsate.com

International Journal of
Science, Architecture, Technology and Environment

Application of the Adaptive Kalman Filter in Sensor Drift Compensation and Accuracy Enhancement of the Inertial Navigation System

Khuat Quang Tien[1*], Vu Van Son[2], Nguyen Ha Giang[2]

[1] *Faculty of Fundamental Technical, Air Defence-Air Force Academy, Ha Noi, Viet Nam*

[2]*Missile Faculty, Air Defence-Air Force Academy, Ha Noi, Viet Nam*

[*]*Corresponding author email: quangtienmta@gmail.com*

DOI: https://doi.org/10.63680/ijsate0726002.2

Abstract

The Inertial Navigation System (INS) has the advantage of operating independently without relying on external signals; however, it is significantly affected by the accumulated errors from inertial sensors, particularly the drift of gyroscopes and accelerometers. This paper presents a simulation and performance evaluation method for the INS with a model including the states of position, velocity, attitude angles (roll, pitch, yaw), and sensor errors. The Adaptive Kalman Filter (AKF) is applied to simultaneously estimate the system states and errors, allowing dynamic updating of measurement noise characteristics and time-varying sensor drift compensation. Simulation results show that the filter significantly improves trajectory and attitude estimation accuracy while minimizing long-term accumulated errors. The proposed method demonstrates high applicability in aerospace and autonomous vehicle systems.

Keywords: Inertial Navigation System; Kalman Filter, Adaptive Kalman Filter, Attitude angles, Error estimation, Sensor drift compensation.

1. Introduction

The INS is a key component in aviation, aerospace, and autonomous vehicles due to its ability to operate independently without external aiding signals such as GPS. However, its main limitation lies in the accumulation of errors over time, primarily caused by gyroscope drift, accelerometer bias, and zero-offset variations. These errors lead to significant deviations in estimating position, velocity, and especially attitude angles (roll, pitch, yaw) of the moving body.

To mitigate these errors, many studies have applied the Kalman Filter (KF) to combine dynamic models with sensor measurements, improving state estimation accuracy. However, in practical conditions, measurement noise often varies over time, reducing the effectiveness of the classical KF. Therefore, applying an AKF becomes essential, as it allows dynamic adjustment of the measurement noise covariance matrix, thereby improving estimation capability and compensating for sensor drift.

This paper focuses on constructing a simulation model of an INS integrated with the AKF. The proposed method enables simultaneous estimation of key system states such as position, velocity, attitude angles, and sensor errors. Through the dynamic update mechanism of the measurement noise matrix, the AKF can correct the drift of gyroscopes and accelerometers during operation, thereby enhancing estimation accuracy. The effectiveness of the proposed method is evaluated using quantitative metrics including MAE, RMSE, BIAS, and STD, demonstrating strong potential for application in aerospace and

modern autonomous systems.

2. Algorithm Synthesis

The AKF algorithm is synthesized for the INS. The model is constructed based on a state vector consisting of position, velocity, attitude angles (roll, pitch, yaw), gyroscope bias, and accelerometer bias. The algorithm is organized into three main blocks: the state model, the measurement model, and the adaptive filtering process.

2.1. State Model

The INS can be represented by the discrete-time linear state-space model:

$$\boldsymbol{x}_{k+1} = \boldsymbol{F}_k \boldsymbol{x}_k + \boldsymbol{G}_k \mathbf{w}_k \quad (1)$$

Where:

$\boldsymbol{x}_k$ is the state vector at time step k;

$\boldsymbol{F}_k$ is the state transition matrix;

$\boldsymbol{G}_k$ is the process noise transition matrix;

$\mathbf{w}_k$ is Gaussian process noise with covariance $\boldsymbol{Q}_k = E\left[\mathbf{w}_k \mathbf{w}_k^T\right]$.

The general form of the state vector is:

$$\boldsymbol{x}(k) = \begin{bmatrix} \boldsymbol{p}(k) \\ \boldsymbol{v}(k) \\ \boldsymbol{\vartheta}(k) \\ \boldsymbol{b}_g(k) \\ \boldsymbol{b}_a(k) \end{bmatrix} \quad (2)$$

Where:

$\boldsymbol{p}(k) = \begin{bmatrix} p_E & p_N & p_U \end{bmatrix}^T$ position components along East, North, and Up axes (m);

$\boldsymbol{v}(k) = \begin{bmatrix} v_E & v_N & v_U \end{bmatrix}^T$ corresponding velocity components (m/s);

$\boldsymbol{\vartheta}(k) = \begin{bmatrix} \phi & \theta & \psi \end{bmatrix}^T$ attitude angles (roll, pitch, yaw) (deg);

$\boldsymbol{b}_g(k) = \begin{bmatrix} b_{gx} & b_{gy} & b_{gz} \end{bmatrix}^T$ gyroscope bias (deg/s);

$\boldsymbol{b}_a(k) = \begin{bmatrix} b_{ax} & b_{ay} & b_{az} \end{bmatrix}^T$ accelerometer bias (m/s²).

The position kinematics equation is:

$$\dot{\boldsymbol{p}}(t) = \boldsymbol{v}(t) \quad (3)$$

Discretized with sampling interval Δt:

$$\boldsymbol{p}_{k+1} = \boldsymbol{p}_k + \boldsymbol{v}_k \Delta t \quad (4)$$

Velocity dynamics in the navigation frame are influenced by gravity and sensor measurements:

$$\dot{\boldsymbol{v}}(t) = \boldsymbol{C}_b^n(t)\left[\boldsymbol{f}_b(t) - \boldsymbol{b}_a(t)\right] + \boldsymbol{g}_n \quad (5)$$

Where:

$\boldsymbol{C}_b^n$ is the direction cosine matrix transforming body-frame to navigation-frame coordinates;

$\boldsymbol{f}_b$ is the accelerometer-measured acceleration (m/s²);

$\boldsymbol{b}_a$ is the accelerometer bias (m/s²);

ISSN 3048-8222 (Online) | www.ijsate.com | editor@ijsate.com

$\boldsymbol{g}_n = [0, 0, -g]^T$ is the gravity vector with g=9.81(m/s^2).

Discretizing equation (5) yields:

$$\boldsymbol{v}_{k+1} = \boldsymbol{v}_k + (\boldsymbol{C}_b^n(\boldsymbol{f}_b - \boldsymbol{b}_a) + \boldsymbol{g}_n)\Delta t \tag{6}$$

Attitude angles (roll, pitch, yaw) depend on angular rates measured by the gyroscope:

$$\dot{\boldsymbol{\vartheta}}(t) = \boldsymbol{T}(\boldsymbol{\vartheta})(\boldsymbol{\omega}_b(t) - \boldsymbol{b}_g(t)) \tag{7}$$

$\boldsymbol{\omega}_b = [\omega_x, \omega_y, \omega_z]^T$ is the angular rate measured by the gyroscope (deg/s);

$\boldsymbol{b}_g$ is the gyroscope bias (deg/s);

$\boldsymbol{T}(\boldsymbol{\vartheta})$ is the transformation matrix from angular velocity to Euler angle rates:

$$\boldsymbol{T}(\boldsymbol{\vartheta}) = \begin{bmatrix} 1 & \sin\phi\tan\theta & \cos\phi\tan\theta \\ 0 & \cos\phi & -\sin\phi \\ 0 & \dfrac{\sin\phi}{\cos\theta} & \dfrac{\cos\phi}{\cos\theta} \end{bmatrix} \tag{8}$$

Discrete form:

$$\boldsymbol{\vartheta}_{k+1} = \boldsymbol{\vartheta}_k + \boldsymbol{T}(\boldsymbol{\vartheta}_k)(\boldsymbol{\omega}_b - \boldsymbol{b}_g)\Delta t \tag{9}$$

Gyroscope and accelerometer biases are commonly modeled as first-order Markov processes:

$$\dot{\boldsymbol{b}}_g = -\frac{1}{\tau_g}\boldsymbol{b}_g + \boldsymbol{w}_g \tag{10}$$

$$\dot{\boldsymbol{b}}_a = -\frac{1}{\tau_a}\boldsymbol{b}_a + \boldsymbol{w}_a \tag{11}$$

τ_g, τ_a are the time constants of the sensor bias processes (s);

$\boldsymbol{w}_g$, $\boldsymbol{w}_a$ are white Gaussian noises characterizing the random variations of sensor biases.

Discretizing equations (10) and (11) gives:

$$\boldsymbol{b}_{g,k+1} = (1 - \frac{\Delta t}{\tau_g})\boldsymbol{b}_{g,k} + \boldsymbol{w}_{g,k} \tag{12}$$

$$\boldsymbol{b}_{a,k+1} = (1 - \frac{\Delta t}{\tau_a})\boldsymbol{b}_{a,k} + \boldsymbol{w}_{a,k} \tag{13}$$

From the above, the state transition matrix $\boldsymbol{F}$ can be written as:

$$\boldsymbol{F} = \begin{bmatrix} \boldsymbol{I}_3 & \Delta t\boldsymbol{I}_3 & 0 & 0 & 0 \\ 0 & \boldsymbol{I}_3 & \boldsymbol{A}_{va} & 0 & -\boldsymbol{C}_b^n\Delta t \\ 0 & 0 & (1 - \dfrac{\Delta t}{\tau_\vartheta})\boldsymbol{I}_3 & -\boldsymbol{T}(\boldsymbol{\vartheta})\Delta t & 0 \\ 0 & 0 & 0 & (1 - \dfrac{\Delta t}{\tau_g})\boldsymbol{I}_3 & 0 \\ 0 & 0 & 0 & 0 & (1 - \dfrac{\Delta t}{\tau_a})\boldsymbol{I}_3 \end{bmatrix} \tag{14}$$

τ_ϑ, τ_g, τ_a are the time constants characterizing the decay of biases in each state group.

$\boldsymbol{A}_{va}$ is the coupling between attitude and velocity due to gravity.

Off-diagonal blocks describe correlations between position–velocity–attitude.

ISSN 3048-8222 (Online) | www.ijsate.com | editor@ijsate.com

2.2. Measurement model

The system measurement signals include quantities of position, velocity and attitude observed at time k, described by the linear equation:

$$\boldsymbol{z}_k = \boldsymbol{H}\boldsymbol{x}_k + \boldsymbol{v}_k \tag{15}$$

Where $\boldsymbol{z}_k$ is the 9×1 measurement vector; $\boldsymbol{H}$ is the 9×15 measurement matrix.

The matrix $\boldsymbol{H}$ has a block form:

$$\boldsymbol{H} = \begin{bmatrix} \boldsymbol{I}_3 & \boldsymbol{0}_3 & \boldsymbol{0}_3 & \boldsymbol{0}_3 & \boldsymbol{0}_3 \\ \boldsymbol{0}_3 & \boldsymbol{I}_3 & \boldsymbol{0}_3 & \boldsymbol{0}_3 & \boldsymbol{0}_3 \\ \boldsymbol{0}_3 & \boldsymbol{0}_3 & \boldsymbol{I}_3 & \boldsymbol{0}_3 & \boldsymbol{0}_3 \end{bmatrix} \tag{16}$$

Measurement noise $\boldsymbol{v}_k \sim N(0, \boldsymbol{R}_k)$ is Gaussian with covariance matrix $\boldsymbol{R}_k = diag(\sigma_p^2, \sigma_v^2, \sigma_\theta^2)$ where $\sigma_p, \sigma_v, \sigma_\theta$ are the standard deviations of position (m), velocity (m/s) and attitude (deg) measurements, respectively.

2.3. Adaptive Kalman Filter Algorithm

The adaptive Kalman filter is used to simultaneously estimate the system states and errors. The algorithm comprises two main stages: prediction and update, presented as follows:

Prediction stage:

- System dynamics used to predict the a priori state estimate:

$$\hat{\boldsymbol{x}}_{k|k-1} = \boldsymbol{F}\hat{\boldsymbol{x}}_{k-1|k-1} \tag{17}$$

- Predicted error covariance matrix:

$$\boldsymbol{P}_{k|k-1} = \boldsymbol{F}\boldsymbol{P}_{k-1|k-1}\boldsymbol{F}^T + \boldsymbol{Q} \tag{18}$$

Update stage:

- Innovation (measurement residual):

$$\boldsymbol{y}_k = \boldsymbol{z}_k - \boldsymbol{H}\hat{\boldsymbol{x}}_{k|k-1} \tag{19}$$

- Innovation covariance:

$$\boldsymbol{S}_k = \boldsymbol{H}\boldsymbol{P}_{k|k-1}\boldsymbol{H}^T + \boldsymbol{R}_k \tag{20}$$

- Kalman gain:

$$\boldsymbol{K}_k = \boldsymbol{P}_{k|k-1}\boldsymbol{H}^T\boldsymbol{S}_k^{-1} \tag{21}$$

- Corrected state estimate:

$$\hat{\boldsymbol{x}}_{k|k} = \hat{\boldsymbol{x}}_{k|k-1} + \boldsymbol{K}_k\boldsymbol{y}_k \tag{22}$$

- Posterior error covariance:

$$\boldsymbol{P}_{k|k-1} = (\boldsymbol{I} - \boldsymbol{K}_k\boldsymbol{H})\boldsymbol{P}_{k|k-1} \tag{23}$$

To ensure adaptability to changes in measurement noise in practice, the matrix $\boldsymbol{R}_k$ is updated dynamically based on the statistics of the innovation sequence:

$$\boldsymbol{R}_k = (1-\alpha_R)\boldsymbol{R}_{k-1} + \alpha_R\bar{\boldsymbol{C}}_y(k) \tag{24}$$

α_R is the smoothing coefficient $0 < \alpha_R < 1$.

$\bar{\boldsymbol{C}}_y(k)$ is the sample covariance of the innovations within a window N_{W}.

ISSN 3048-8222 (Online) | www.ijsate.com | editor@ijsate.com

$$\hat{\boldsymbol{C}}_y(k) = \frac{1}{N_{\mathrm{W}} - 1} \sum_{i=k-N_{\mathrm{W}}+1}^{k} (\boldsymbol{y}_i - \bar{\boldsymbol{y}})(\boldsymbol{y}_i - \bar{\boldsymbol{y}})^T \tag{25}$$

With $\bar{\boldsymbol{y}}$ being the sample mean of innovations in the window.

This dynamic update mechanism enables the filter to self-adjust the measurement noise covariance matrix according to real conditions, ensuring stability and high adaptability under time-varying measurement noise.

2.4. Filter performance evaluation

To evaluate the performance of the AKF in estimating states and correcting sensor drift, common quantitative metrics used include Mean Absolute Error (MAE), Root Mean Square Error (RMSE), Mean Bias (BIAS), Standard Deviation (STD) and Jitter. These metrics reflect accuracy, stability and remaining noise in the estimated signals.

Assume $\hat{x}_i$ is the estimated value of a state variable at sample i, x_i s the true (or reference) value, and N is the total number of samples; the metrics are computed as follows:

Mean Absolute Error:

$$MAE = \frac{1}{N} \sum_{i=1}^{N} \left| x_i - \hat{x}_i \right| \tag{26}$$

The MAE metric indicates the average absolute difference between the true value and the estimated value. The smaller the MAE, the more accurate the filter.

Root Mean Square Error:

$$RMSE = \sqrt{\frac{1}{N} \sum_{i=1}^{N} \left(x_i - \hat{x}_i \right)^2} \tag{27}$$

RMSE emphasizes larger errors because of the squaring before averaging. A small RMSE indicates low dispersion of errors and high accuracy.

Mean Bias:

$$BIAS = \frac{1}{N} \sum_{i=1}^{N} \left(x_i - \hat{x}_i \right) \tag{28}$$

BIAS reflects the systematic offset tendency of the filter. If BIAS ≈ 0, the filter is unbiased; if BIAS ≠ 0, filter parameters or the noise model need adjustment.

Standard Deviation of the error (STD):

$$STD = \sqrt{\frac{1}{N} \sum_{i=1}^{N} [\left(x_i - \hat{x}_i \right) - BIAS]^2} \tag{29}$$

STD indicates the fluctuation level of the error around its mean. The smaller the STD, the more stable and reliable the filter.

Jitter:

$$Jitter = \sqrt{\frac{1}{N-1} \sum_{i=2}^{N} \left[(\hat{x}_i - \hat{x}_{i-1}) - \frac{1}{N-1} \sum_{j=2}^{N} (\hat{x}_j - \hat{x}_{j-1}) \right]^2} \tag{30}$$

Where:

i is the sample index considered in the estimated value sequence $\hat{x}_i$.

j is an intermediate index used in computing the mean of all consecutive differences.

Jitter characterizes the short-term variability of the estimated value between consecutive samples, reflecting the instantaneous stability of the filter. This metric is computed as the variance of the rate of

ISSN 3048-8222 (Online) | www.ijsate.com | editor@ijsate.com

change of the estimated values.

3. Simulation and Evaluation

To verify the ability of sensor drift correction and the improvement of estimation accuracy in the INS, the simulation model is developed based on the application of the AKF. The filter is designed to simultaneously estimate the position, velocity, attitude angles, and sensor errors of both gyroscopes and accelerometers.

During the simulation, the drift and noise characteristics of the sensors are modeled as first-order Markov processes, accurately representing the random deviations and the accumulated error tendency of the INS under real operating conditions. The measurement noise is simulated as time-varying, allowing the AKF to dynamically adjust the measurement noise matrix $\boldsymbol{R}_k$ based on the innovation statistics. This mechanism enables the filter to flexibly respond to changes in the signal and maintain high stability during estimation.

The simulation parameters are selected based on the characteristics of mid-grade inertial sensors to properly reflect the influence of drift and noise during operation. The measurement noise is modeled as time-varying to verify the adaptability of the filter. The simulation parameters are selected as follows:

- Simulation time: 100 (s);
- Sampling period: $\Delta t = 100$;
- Gravity: $g = 9.81(m/s^2)$;
- Dimensions of state and measurement vectors: $n_x = 15, n_z = 9$;
- Dynamic time constants: $\tau_\phi = \tau_\theta = \tau_\psi = 50(s);\ \tau_g = 20(s);\ \tau_a = 30(s);$
- Process noise matrix: $\boldsymbol{Q} = diag(\boldsymbol{Q}_p, \boldsymbol{Q}_v, \boldsymbol{Q}_{att}, \boldsymbol{Q}_{bg}, \boldsymbol{Q}_{ba})$;

Where:

$\boldsymbol{Q}_p = diag(0.05^2, 0.05^2, 0.05^2)(m^2)$

$\boldsymbol{Q}_v = diag(10^{-3}, 10^{-3}, 10^{-3})(m/s)^2$

$\boldsymbol{Q}_{att} = diag(10^{-6}, 10^{-6}, 10^{-6})(\deg^2)$

$\boldsymbol{Q}_{bg} = diag(10^{-7}, 10^{-7}, 10^{-7})(\deg/s)^2$

$\boldsymbol{Q}_{ba} = diag(0.05^2, 0.05^2, 0.05^2)(m/s^2)^2$

- Measurement noise matrix: $\boldsymbol{R}_k = diag(\boldsymbol{R}_p, \boldsymbol{R}_v, \boldsymbol{R}_{att})$;

Where:

$\boldsymbol{R}_p = diag(1^2, 1^2, 1^2)(m^2)$

$\boldsymbol{R}_v = diag(0.5^2, 0.5^2, 0.5^2)(m/s)^2$

$\boldsymbol{R}_{att} = diag(10^{-4}, 10^{-4}, 10^{-4})(\deg)^2$

- Initial covariance matrix: $\boldsymbol{P}_0 = diag(\boldsymbol{P}_p, \boldsymbol{P}_v, \boldsymbol{P}_{att}, \boldsymbol{P}_{bg}, \boldsymbol{P}_{ba})$;

Where:

$\boldsymbol{P}_p = diag(50, 50, 50)(m^2)$

$\boldsymbol{P}_v = diag(5, 5, 5)(m/s)^2$

$\boldsymbol{P}_{att} = diag(2^2, 2^2, 3^2)(\deg)^2$

$\boldsymbol{P}_{bg} = diag(0.05, 0.05, 0.05)(\deg/s)^2$

$\boldsymbol{P}_{ba} = diag(0.1^2, 0.1^2, 0.1^2)(m/s^2)^2$

- Sliding window size: $N_w = 20$;
- Smoothing coefficient: $\alpha_R = 0.05$.

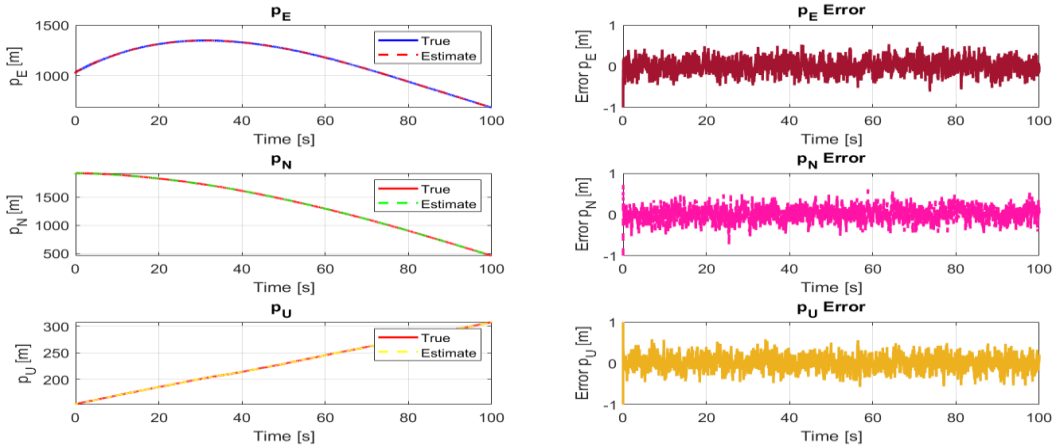

Figure 1. Estimated position and position error results

Figure 1 presents the estimated position results in three components: East (p_E), North (p_N) and Up (p_U) of the inertial navigation system using the AKF during 100 (s) of simulation. The results show that the estimated components are highly accurate, and the estimation curves almost overlap the true trajectories throughout the simulation, indicating fast and stable convergence of the filter.

The position errors in all three axes fluctuate slightly around the zero mean with amplitudes within ±1 (m). The RMSE values of the position components are approximately $RMSE(p_E) \approx 0.45(m)$, $RMSE(p_N) \approx 0.47(m)$ and $RMSE(p_N) \approx 0.42(m)$, all below 0.5 (m). The Up component p_U shows slightly larger fluctuations due to the direct influence of vertical accelerometer bias. The results in Figure 1 confirm that the AKF allows the system to accurately estimate the spatial trajectory, with position errors maintained below 1 m throughout the entire simulation, ensuring high stability and reliability for the INS model.

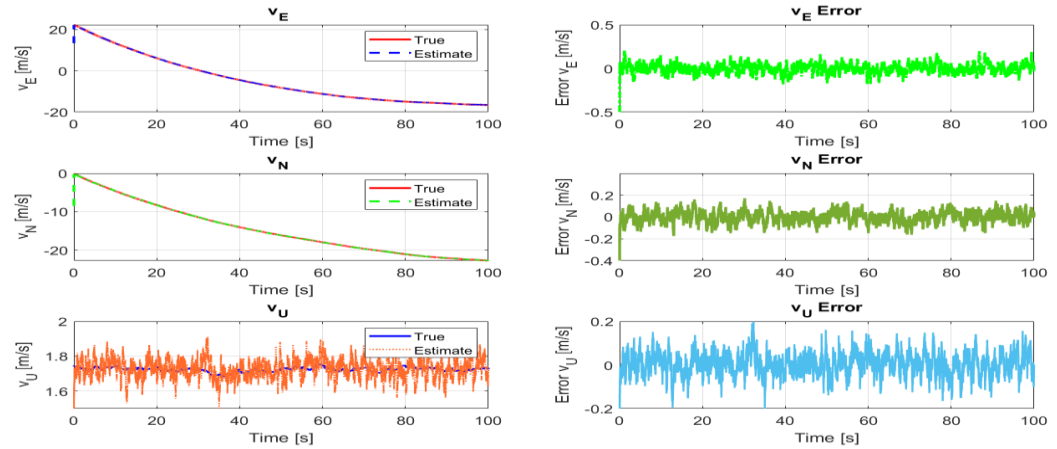

Figure 2. Estimated velocity and velocity error results

The results show that the velocity components are accurately estimated, with the estimated curves almost coinciding with the true values during the entire simulation. The velocity errors in the three axes fluctuate around zero mean without any drift trend, demonstrating the stability of the filter. The maximum error amplitudes of V_E, V_N, V_U are within ±0.5 (m/s). The RMSE values are $RMSE(V_E) \approx 0.18(m/s)$,

ISSN 3048-8222 (Online) | www.ijsate.com | editor@ijsate.com

$RMSE(V_N) \approx 0.16(m/s)$ and $RMSE(V_U) \approx 0.14(m/s)$, all less than 0.2 (m/s). These results confirm that the AKF effectively compensates for velocity noise and accurately estimates the system's linear dynamic states, ensuring high reliability during deceleration and steady-state motion.

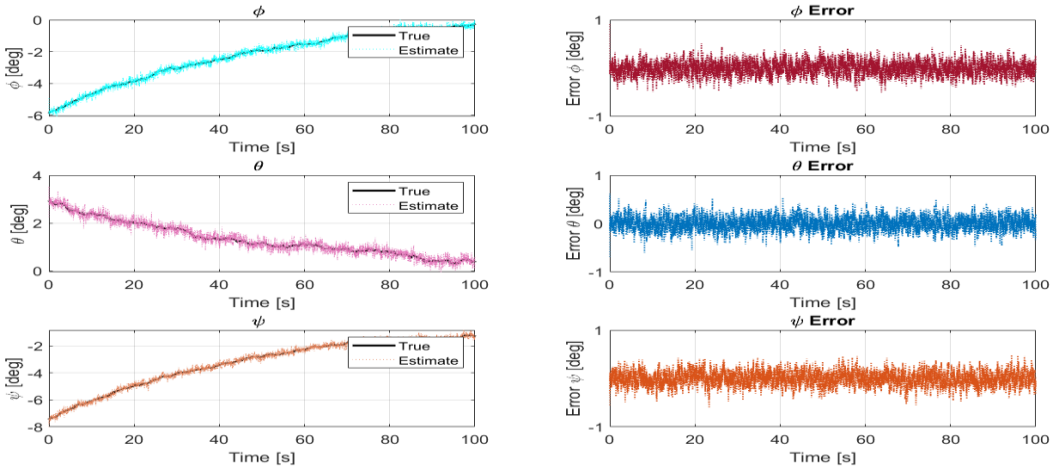

Figure 3. Estimated attitude angles and attitude error results

Figure 3 illustrates the estimation results of the three attitude angles: roll (φ), pitch (θ), and yaw (ψ) of the INS using the AKF. The estimated attitude angles closely match the true values during the entire simulation. The estimation errors oscillate slightly around zero without angular drift, demonstrating the stability and adaptability of the filter under sensor noise.

The maximum error amplitudes of the attitude angles are within ±1 (deg). The RMSE values are $RMSE(\phi) \approx 0.35(\text{deg})$, $RMSE(\theta) \approx 0.32(\text{deg})$ and $RMSE(\psi) \approx 0.38(\text{deg})$, indicating that the filter accurately estimates rotational states while maintaining smoothness and stability. The results in Figure 3 confirm that the AKF not only reduces instantaneous angular errors but also ensures reliable estimation of attitude parameters in the INS during the entire simulation.

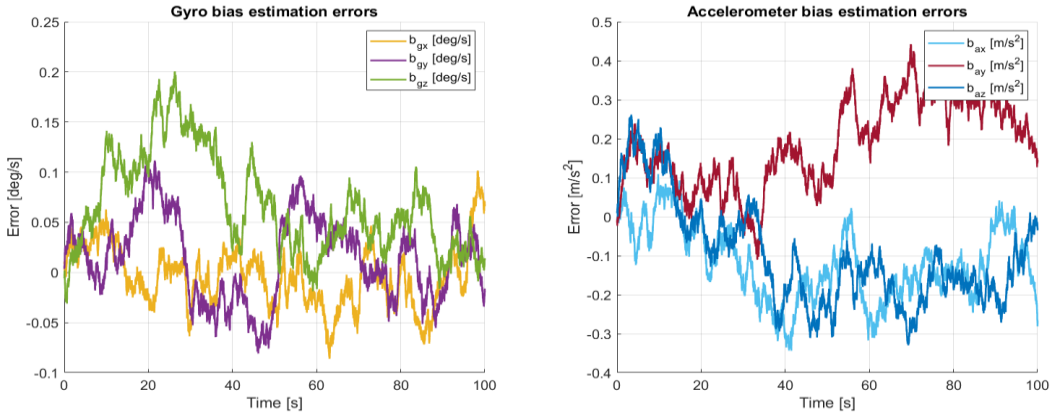

Figure 4. Estimated gyroscope and accelerometer bias errors

Figure 4 shows the estimated errors of sensor biases, including gyroscope drift (b_{gx}, b_{gy}, b_{gz}) and accelerometer drift (b_{ax}, b_{ay}, b_{az}) throughout the 100 (s) simulation. The estimated gyroscope bias errors fluctuate slightly around zero with amplitudes below ±0.1 (deg/s), proving that the filter accurately tracks and compensates gyroscope angular drift.

The accelerometer bias errors vary within ±0.3 (m/s^2), demonstrating the adaptability of the filter in correcting slowly varying accelerometer biases. Both groups of errors show no accumulation trend, indicating stable and reliable estimation performance.

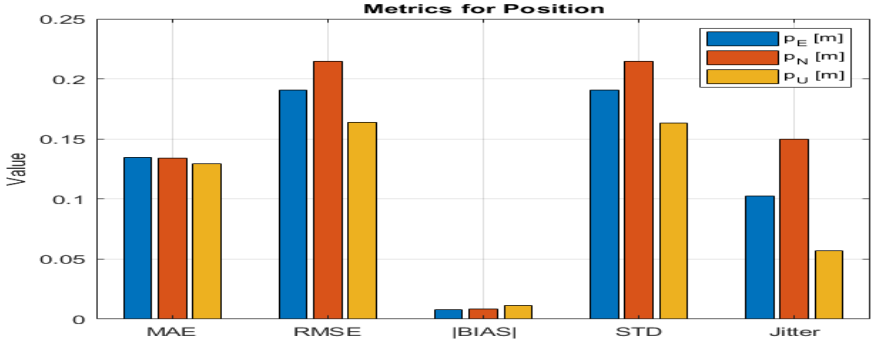

Figure 5. Quantitative indices of position estimation errors

Figure 5 presents the quantitative indices evaluating position estimation performance along the East–North–Up axes (p_E, p_N, p_U), including MAE, RMSE, |BIAS|, STD and Jitter. The RMSE values of the position components are 0.19 (m), 0.22 (m), and 0.17 (m), while MAE values are around 0.13 (m). The |BIAS| values are all less than 0.02 (m), and the standard deviation (STD) remains within 0.15–0.2 (m). This proves that position errors are effectively controlled and the filter achieves accurate estimation even under position measurement noise with variance 1^2 (m^2). The small Jitter (Jitter < 0.2 m) confirms that the output signals are stable and exhibit low random fluctuations.

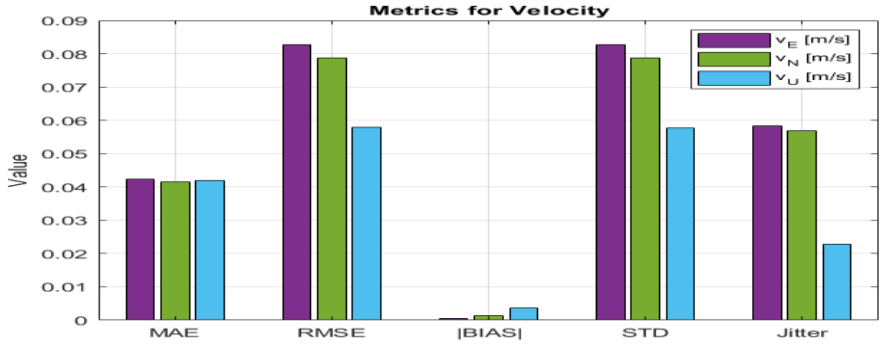

Figure 6. Quantitative indices of velocity estimation errors

Figure 6 illustrates the filter performance indices for velocity states (V_E, V_N, V_U). The RMSE values are 0.083 (m/s), 0.079 (m/s) and 0.058 (m/s), while MAE values range from 0.04–0.05 (m/s). The average |BIAS| is less than 0.01 (m/s) and STD < 0.08 (m/s), reflecting high stability of the filter in velocity estimation. The results match the measurement noise variance of 0.5^2 (m/s)^2. The small Jitter indicates that the AKF output is smooth without oscillations, ensuring reliability in tracking dynamic motions.

ISSN 3048-8222 (Online) | www.ijsate.com | editor@ijsate.com

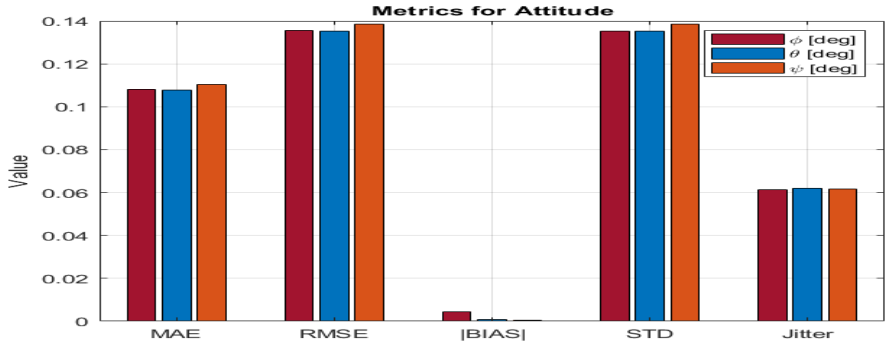

Figure 7. Quantitative indices of attitude angle estimation errors

Figure 7 presents quantitative indices (MAE, RMSE, |BIAS|, STD, Jitter) for the three attitude angles of the INS. The average MAE and RMSE values are both very small, below 0.12 (deg) and 0.14 (deg) respectively, indicating high accuracy of attitude estimation. The |BIAS| values are close to zero, confirming that the filter remains unbiased and maintains long-term stability. The STD values of the three attitude angles are approximately 0.14 (deg), showing low fluctuation and stable distribution around the mean. The Jitter index is also low (< 0.065 deg), reflecting smooth attitude estimation with minimal short-term oscillations. Therefore, the AKF ensures accurate and stable estimation of the system's rotational states, enhancing the reliability of the INS throughout the simulation.

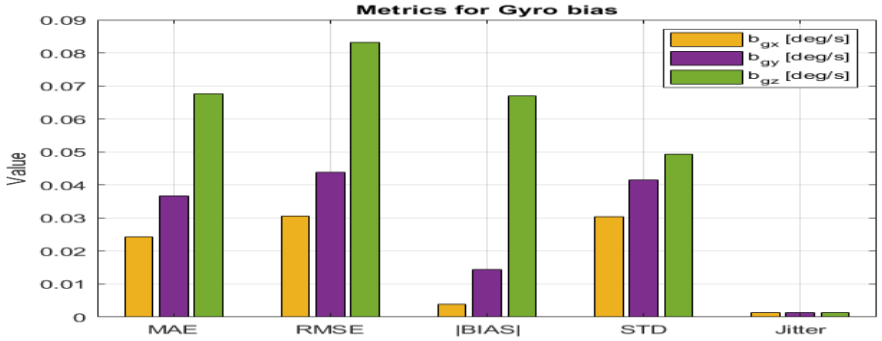

Figure 8. Quantitative indices of gyroscope drift estimation errors

Figure 8 presents the quantitative evaluation of gyroscope drift estimation errors along the three axes. The MAE and RMSE values of all components remain below 0.09 (deg/s), demonstrating the filter's high precision in tracking sensor angular drift. The |BIAS| of all axes is nearly zero, varying slightly within ±0.01 (deg/s), reflecting the filter's capability to eliminate directional bias. The STD is low (< 0.07 deg/s), indicating stable and low-variance errors. Additionally, the Jitter index is very small (≈ 0.002 deg/s), confirming that the bias estimation process is smooth without instantaneous fluctuations. Overall, Figure 8 demonstrates that the AKF effectively compensates gyroscope drift, limiting angular accumulation and ensuring long-term stability of the INS.

ISSN 3048-8222 (Online) | www.ijsate.com | editor@ijsate.com

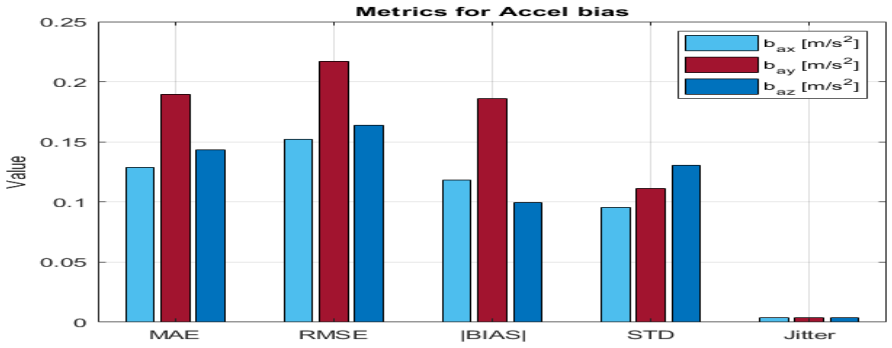

Figure 9. Quantitative indices of accelerometer drift estimation errors

Figure 9 shows the quantitative evaluation of accelerometer drift estimation errors along the three axes. The MAE and RMSE values of all components range from 0.12–0.22 (m/s^2), with the y-axis component being the largest due to higher random noise influence. The |BIAS| values are all less than 0.18 (m/s^2), and the STD ranges from 0.09–0.12 (m/s^2), indicating stable errors without long-term drift. The Jitter index is very small (≈ 0.004 m/s^2), reflecting stable and smooth estimated signals. The results in Figure 9 confirm that the AKF efficiently estimates and compensates slow-varying accelerometer biases, thereby improving the overall accuracy of the inertial navigation system.

4. Conclusion

This paper has presented the simulation method and performance evaluation of the Adaptive Kalman Filter (AKF) in state estimation and sensor drift correction for the Inertial Navigation System (INS). Based on a complete state model including position, velocity, attitude angles (roll, pitch, yaw), and sensor biases (gyroscope and accelerometer), the AKF was designed to allow dynamic updating of the measurement noise covariance matrix, enabling adaptation to time-varying measurement noise conditions in practice.

The simulation results show that the AKF significantly improves the accuracy of the INS compared to the classical Kalman Filter. Specifically, the position estimation error remains below 1 (m), the velocity error is less than 0.2 (m/s), and the attitude angle error is under 0.5 (deg), ensuring stability and fast convergence. Quantitative indicators such as MAE, RMSE, |BIAS|, STD, and Jitter all exhibit small and stable values, proving that the estimated signals are smooth, exhibit minimal fluctuation, and are free from systematic bias.

In addition, the filter's capability in tracking and compensating sensor drift is clearly demonstrated through the results for gyroscope and accelerometer biases, where the bias errors are maintained around zero mean without any accumulation tendency. The obtained results confirm that the Adaptive Kalman Filter is an effective solution for enhancing the accuracy and reliability of the Inertial Navigation System, particularly under varying or uncertain measurement noise conditions. This approach can be extended to applications in aerospace, unmanned aerial vehicles (UAVs), and integrated inertial/GNSS navigation systems. In the future, further research directions may focus on combining the AKF with machine learning techniques to optimize the parameter adjustment process, as well as implementing real-time experiments on hardware platforms to evaluate the filter performance in actual dynamic environments.

Declaration of Conflicting Interests

The authors declare no potential conflicts of interest with respect to the research, authorship and publication of this article.

Funding

The author received no financial support for the research, authorship and publication of this article.

References

[1] Y. Shi, Y. Zhang, Z. Li, S. Yuan, and S. Zhu, "IMU/UWB fusion method using a complementary filter and a Kalman filter for hybrid upper limb motion estimation," *Sensors*, vol. 23, no. 15, 2023.

[2] O. Uyar, "Performance evaluation of IMU filtering techniques in yaw-pitch-roll calculations," *International Journal of Advanced Natural Sciences and Engineering Researches*, vol. 8, 2024.

[3] A. Liu, H. Guo, M. Yu, J. Xiong, H. Liu, and P. Xie, "Research on GNSS/IMU/Visual fusion positioning based on adaptive filtering," *Applied Sciences*, vol. 14, 2024.

[4] Toan, N. T. (2026). Integration of Multi-Frequency Oscillation Models and Pseudo Linear Acceleration for Advanced IMU Sensor Data Simulation and Attitude Estimation Accuracy Enhancement. International Journal of Science, Architecture, Technology, and Environment, 03(06), 235–244. https://doi.org/10.63680/ijsate062621.21